DOI: 10.1002/cjoc.201600490

High Sensitive Ambipolar Response towards Oxidizing NO_2 and Reducing NH_3 Based on Bis(phthalocyaninato) Europium Semiconductors

Xia Kong,[a] Zhen Dong,[a] Yanling Wu,[a] Xiyou Li,[a] Yanli Chen,*[,a] and Jianzhuang Jiang*[,a,b]

[a] *School of Science*, *China University of Petroleum* (*East China*), *Qingdao*, *Shandong 266580*, *China*
[b] *Beijing Key Laboratory for Science and Application of Functional Molecular and Crystalline Materials*, *Department of Chemistry*, *University of Science and Technology Beijing*, *Beijing 100083*, *China*

High sensitive chemical sensors towards NO_2 and NH_3 based on the self-assembled nanostructures of the heteroleptic and homoleptic bis(phthalocyaninato) europium complexes with octanaphthoxy phthalocyaninato ligands named Eu(Pc)[Pc(ONh)$_8$] (**1**) and Eu[Pc(ONh)$_8$]$_2$ (**2**) [Pc = unsubstituted phthalocyaninate; Pc(ONh)$_8$ = 2,3,9,10,16,17,23,24-octanaphthoxy phthalocyaninate] have been developed. The good conductivity, high crystallinity and large specific surface area for the self-assemblies of **1** render it excellent sensing property for either electron-accepting gas NO_2 in 50－250 ppb range or electron-donating gas NH_3 in 2.5－12.5 ppm range due to the optimized molecular packing in the uniform-sized nanoparticles depending on the effective intermolecular interaction between double-decker molecules, among the best results of phthalocyanine-based chemical sensors for detection of NO_2 and NH_3 at room temperature. Interestingly, self-assemblies of **1** exhibited *n*-type response to NO_2 and *p*-type response to NH_3, which is the first example of ambipolar charge-transporting gas sensors fabricated from single-component organic semiconductors. However, the self-assemblies of **2** with sixteen bulky naphthoxy groups at the periphery of two Pc rings only present an *n*-type response to strong oxidant gas NO_2 in a relatively high concentration of 0.5－1.5 ppm, while are insensitive to weak reducing gas NH_3 due to the existence of great steric hindrance from bulky naphthoxy groups and more traps and/or defects in self-assemblies.

Keywords phthalocyanine, double-decker, gas sensor, self-assemblies, ambipolar semiconductor

Introduction

Among functional molecular materials with large conjugated electronic molecular structures, phthalocyanines (Pcs) have received a particular attention due to their high thermal and chemical stabilities, great processability and rich substitution chemistry, leading to a large flexibility in tuning molecular structures and macroscopic properties.[1] In addition, the electrical conductivity of phthalocyanines, which are mostly *p*-type organic semiconductors, is known to vary substantially in the presence of oxidizing or reducing gases due to the change in charge carrier concentrations upon adsorption of gas molecules.[2,3] These materials have been widely explored as chemiresistive gas sensors since about twenty years ago.[4] For most of the applications, the properties of the molecular devices are closely related to the microstructures of the molecular materials. Many efforts have been made to clarify the relationship between the basic chemical structures, nanostructures self-assembled from Pc-based molecular materials and the device performances. For example, Bouvet *et al*.[5] found that the vacuum evaporated film of *p*-type CoPc with well-organized structure was sensitive to NH_3 and O_3, while the drop-casting film of *n*-type sulfonated CoPc (s-CoPc) with low crystallinity was only sensitive to NH_3. For two typical *n*-type organic semiconductors, F_{16}CuPc and $(CN)_{16}$CuPc, it has been revealed that the vacuum-deposited film of F_{16}CuPc exhibited high organic field-effect transistor (OFET) electron mobility (0.03 $cm^2 \cdot V^{-1} \cdot s^{-1}$) and no OFET behavior was observed for the casting film of $(CN)_{16}$CuPc having poor molecular ordering in the film.[6] However, it must be pointed out that optimizing the intermolecular interaction through the combination of molecular design with morphology-controlled self-assembly to improve sensing performance still remains a great challenge for chemists and material scientists.

Among the large family of the phthalocyanines, double-decker phthalocyanines have been subject to extensive investigations because of their radical nature, excellent molecular semiconducting property and possi-

* E-mail: yanlichen@upc.edu.cn, jianzhuang@ustb.edu.cn
Received August 1, 2016; accepted September 20, 2016; published online XXXX, 2016.
Supporting information for this article is available on the WWW under http://dx.doi.org/10.1002/cjoc. 201600490 or from the author.

ble applications in gas sensing properties.[1,7-10] Very recently, solution-processed thin solid films of bis(phthalocyaninato) holmium double-deckers bearing electron-withdrawing phenoxy substituents at the phthalocyanine periphery Ho(Pc)[Pc(OPh)$_8$] and Ho[Pc(OPh)$_8$]$_2$ have been revealed to display the *p*-type and *n*-type current response to electron-donating gas NH_3 in 15—800 ppm range, respectively.[11] In light of these previous reports, we herein design and prepare the bulky naphthoxy substituted bis(phthalocyaninato) europium semiconductors Eu(Pc)[Pc(ONh)$_8$] (**1**) and Eu[Pc(ONh)$_8$]$_2$ (**2**) [Pc=unsubstituted phthalocyaninate; Pc(ONh)$_8$=2,3,9,10,16,17,23,24-octanaphthoxy phthalocyaninate], Scheme 1. The gas-sensing properties of the self-assembled nanostructures of **1** and **2** fabricated by a solution-processed quasi-Langmuir-Shäfer (QLS) method have been comparatively studied, which confirmed the strong effect of bulky naphthoxy substituents on intermolecular interactions and showed that self-assembled nanostructures of **1** have ambipolar response to both electron-accepting gas NO_2 in 50—250 ppb range and electron-donating gas NH_3 in 2.5—12.5 ppm range at room temperature.

Scheme 1 Schematic molecular structures of bis(phthalocyaninato) europium double-decker complexes EuPc[Pc(ONh)$_8$] (**1**) and Eu[Pc(ONh)$_8$]$_2$ (**2**)

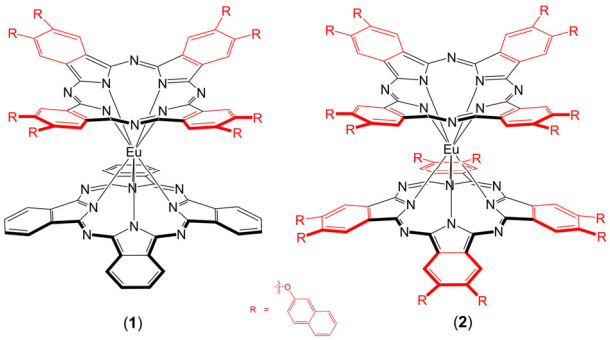

Experimental

Chemicals

1,8-Diazabicyclo[5.4.0]undec-7-ene (DBU) was purchased from Aldrich. The solvent *n*-pentanol was distilled from sodium. DMF for voltammetric study was freshly distilled from CaH_2 under an atmosphere of nitrogen. The compounds of Eu(acac)$_3$•H_2O, EuPc(acac), 4,5-bis(naphthoxy)-1,2-dicyanobenzene were prepared according to the literature methods.[12-15]

Compound characterizations

MALDI–TOF mass spectrum was taken on a Bruker BIFLEX III ultra-high-resolution Fourier transform ion cyclotron resonance (FT–ICR) mass spectrometer with alpha-cyano-4-hydroxycinnamic acid as matrix. ^{1}H NMR spectrum was recorded on a Bruker DPX 400 spectrometer in $CDCl_3$/[D_6]DMSO (1∶1) in the presence of *ca.* 1% (by volume) hydrazine hydrate. Spectrum was referenced internally with residual DMSO (δ 2.49). The electrochemical cell comprised inlets for a glassy carbon disk working electrode of 3.0 mm in diameter and a silver-wire counter electrode. The reference electrode was Ag/Ag$^+$ (a solution of 0.01 mol/L $AgNO_3$ in acetonitrile), which was connected to the solution by a Luggin capillary, whose tip was placed close to the working electrode. Typically, a 0.1 mol•L^{-1} solution of [Bu_4N][ClO_4] as the electrolyte in dried DMF containing 0.5 mmol•L^{-1} of sample was purged with nitrogen for 5 min. After measurement, the result was corrected for junction potentials by being referenced internally to the ferrocenium/ferrocene (Fc$^+$/Fc) couple [$E_{1/2}$(Fc$^+$/Fc)=0.50 V vs. SCE].

Film measurements

For characterizations, self-assemblies were fabricated by QLS method following previously published reference[16] onto the quartz substrate for UV-vis absorption spectra measurement, and onto the bare SiO_2/Si substrate for X-ray diffraction (XRD) and atomic force microscope (AFM) measurements. UV-vis absorption spectra were recorded on a Hitachi U-4100 spectrophotometer. X-ray diffraction experiments were carried out on a Rigaku D/max-B X-ray diffractometer with copper (Kα) radiation (λ=1.5406 Å). Atomic force microscope images were collected under ambient conditions using the tapping mode with a NanoscopeIII/Bioscope scanning probe microscope from digital instruments.

Electrical measurements

The device of gas sensing was fabricated onto the Indium Tin Oxide (ITO) substrate which is composed of 10 pairs of interdigitated electrode array with the following dimensions: 125 mm electrode width, 75 μm spacing, 6000 μm overlapping length, and 20 nm electrode thickness. The fundamental electrical and sensor measurements were performed using a Keysight B2910A precision source/measure unit with an incorporated direct current voltage supply. The electrometer was controlled by Quick IV Measurement Software. Current-voltage (*I-V*) curves were registered in the voltage range of –10—+10 V. And for gas sensing experiments, the samples were constantly polarized at +5 V. All experiments have been conducted at least twice to ensure reproducibility.

Conductivity, σ, obtained by current-voltage (*I-V*) curves can be calculated by the following equation,[17]

$$\sigma=\frac{dI}{(2n-1)LhV} \quad (1)$$

where *d* is the interelectrode spacing, *I* the current, *n* the number of electrode digits, *L* the overlapping length of the electrodes, and *h* the electrode thickness as the film thickness exceeds that of the ITO electrodes in present case.

Flow system for chemical sensing

Sensing experiments were carried out in a cuboid Teflon sensor chamber (*ca.* 30 cm^3 as internal volume). The desired NO_2 or NH_3 concentrations were produced by diluting a mixture NO_2/N_2 (50 ppm NO_2, from Qingdao Ludong Gas., Ltd, China) or NH_3/N_2 (500 ppm NH_3, from Qingdao Ludong Gas., Ltd, China) with dry N_2 using two CS200 Mass Flow Controllers (total mass flow: 0.1 L•min^{-1} for NO_2 or NH_3 and 2 L•min^{-1} for diluent gas N_2), respectively. All tests consisted of the exposure of the sensor to "a static atmosphere" followed by exposure to a known concentration of NO_2 or NH_3.

Results and Discussion

Synthesis and characterizations

The heteroleptic bis(phthalocyninato) rare earth complexes are usually prepared by the treatment of a rare earth acetate with two different lithium phthalocyaninates. To facilitate the synthetic yield and purification, EuPc[Pc(ONh)$_8$] (**1**) was obtained by cyclic tetramerization of the 4,5-bis(naphthoxy)-1,2-dicyanobenzene with the half-sandwich compound Eu(Pc)(acac) as the template in refluxing *n*-pentanol in the presence of 1,8-diazabicyclo[5.4.0]undec-7-ene (DBU) according to the literature methods.[13] A mixture of EuPc(acac) (91.4 mg), and 4,5-bis(naphthoxy)-1,2-dicyanobenzene (238 mg) in *n*-pentanol (3 mL) was refluxed for 3 h under a slow stream of nitrogen. After being cooled to room temperature, 20 mL *n*-hexane was added to the reactor. After standing for 6 h, the precipitate was filtered off, and then washed with *n*-hexane. The residue left was chromatographed on a silica gel column. Due to the poor solubility, a few drops of CH_3OH must be added to the pure $CHCl_3$ [$V(CHCl_3)/V(CH_3OH) = 99 : 1$] as eluent. Repeated chromatography followed by recrystallization from $CHCl_3$ and *n*-hexane gave pure compound of green powder. Yield: 68 mg (30%). ^{1}H NMR (400 MHz, $CDCl_3$) δ: 11.32 (s, 8H, Pc-H$_\alpha$), 10.81 (s, 8H, Pc*-H$_\alpha$), 8.76－8.74 (s, 8H, Pc*-H$_\beta$), 8.76 (s, 8H, Pc*-Nh-H$_{\beta1}$), 8.63 (d, J=11.2 Hz, 8H, Pc-Nh-H$_{\beta2}$), 8.55 (t, J=11.2 Hz, 16H, Pc-Nh-H$_{\beta3,\beta4}$), 8.47 (d, J=16.0 Hz, 8H, Pc-Nh-H$_{\beta7}$), 7.74 (d, J=2.0 Hz, 16H, Pc-Nh-H$_{\beta5,\beta6}$). This newly prepared double-decker compound was characterized by MALDI-TOF spectrum with an isotopic cluster peaking at *m*/*z* 2314, Figure S1, similar with the Calcd result for $C_{144}H_{80}EuN_{16}O_8$, $[MH]^+$, 2314.

The homoleptic bis(phthalocyaninato) rare earth(III) complex Eu[Pc(ONh)$_8$]$_2$ (**2**) was synthesized by the self-cyclic tetramerization of phthalonitriles in the presence of metal salts according to the previously published procedures.[13,14] All other reagents and solvents were of reagent grade and used as received.

Electrochemical properties

The electrochemical behaviors of both double-decker complexes were investigated by differential pulse voltammetry (DPV) in DMF. The double-decker complexes of **1**－**2** displayed one or two quasi reversible one-electron oxidation(s) and three quasi reversible one-electron reductions within the electrochemical window of DMF, Figure 1 and Table S1 (Support Information). The first oxidation and the first reduction processes involve the removal of an electron from and the addition of an electron to the singly occupied molecular orbital, respectively. It is found that the half-wave potentials of the first oxidation as well as the first and second reductions of two compounds correlate with the number of the peripheral octanaphthoxy substituents, which are shifted in the anodic direction along with the increase of the number of octanaphthoxy substituents from **1** to **2**, indicating that incorporation of the sixteen naphthoxy groups on two phthalocyanine rings makes Eu[Pc(ONh)$_8$]$_2$ (**2**) slightly harder to oxidize and easier to reduce than the analogous compound Eu(Pc)-[Pc(ONh)$_8$] (**1**) with eight naphthoxy groups on the phthalocyanine ring. These results are consistent with those findings for the phenoxy and thiophenoxy-substituted bis(phthalocyaninato) metal complexes[13] and octyloxycarbonyl-, F- and CN-substituted phthalocyaninato metal complexes,[18] which clearly reveal the electron-withdrawing nature of these naphthoxy substituents on the phthalocyaninato ligand. In the present

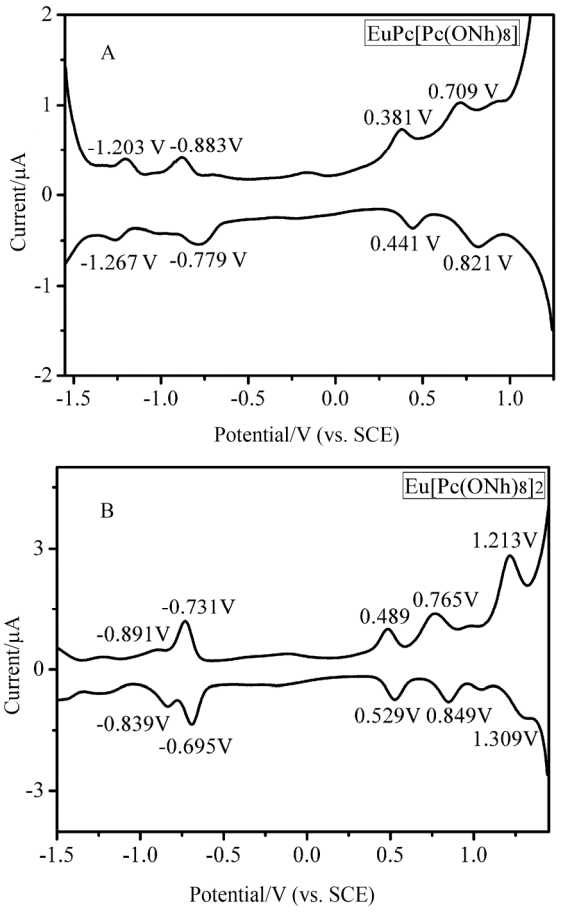

Figure 1 Differential pulse voltammetry (DPV) of **1** (A) and **2** (B) in DMF containing 0.1 mol•L^{-1} [Bu_4N][ClO_4] at a scan rate of 20 mV/s vs. SCE.

case, the HOMO and LUMO energy levels of **1**—**2** were estimated to be about –4.85 and –3.61 eV for **1** and –4.95 and –3.73 eV for **2**, on the basis of their half-wave potentials of the first and second reductions (vs. SCE).[11,19,20] The HOMO and LUMO energies of **1**—**2** just simultaneously meet the energy range required for *p*-type and *n*-type organic semiconductors,[21-23] suggesting the ambipolar organic semiconducting nature of these double-decker complexes.

Film morphologies and microstructures

The self-assemblies of EuPc[Pc(ONh)$_8$] (**1**) and Eu[Pc(ONh)$_8$]$_2$ (**2**) were prepared by a solution-based QLS method.[16,25] The quality of the self-assemblies could be assessed using UV-vis absorption spectra, X-ray diffraction pattern (XRD), and atomic force microscopy (AFM) techniques. As shown in Figure 2, typical UV-vis absorption spectra of heteroleptic and homoleptic bis(phthalocyaninato) rare earth(III) complexes were observed, with the peaks in the 470—490 nm region associated with a free radical structure of rare earth bisphthalocyanines.[11,26] The spectra also show the intense Soret bands in the range of 320—360 nm, and a Q-band, the most intense, at 675 nm for **1**, and 680 nm for **2**, which has been attributed to a π-π* transition, respectively. With the comparision of heteroleptic compound **1** in solution, slightly red-shifts take place in both Q and Soret bands for the naphthoxy-substituted homoleptic double-decker compound **2**. This result is in line with the behavior found from heteroleptic and homoleptic bis(phthalocyaninato) holmium(III) counterparts attaching phenoxy substituents with a slight electron-withdrawing nature.[11,13] Obviously, these optical transitions have a significant contribution from the frontier molecular orbitals delocalized mainly on the two Pc rings, which makes them more susceptible to functionalization by attaching electron-withdrawing groups to the conjugated Pc cores.[11,27] However, after being fabricated into the self-assemblies, the main Q bands were broadened and red-shifted from 675 to 679 nm for **1** and from 680 to 686 nm for **2**, similarly the Soret bands were also red-shifted to 329 nm and 331 nm, respectively. On the basis of Kasha's exciton theory,[28] red shift in the main absorption bands of self-assemblies is a typical sign of that the double-decker molecules are enforced to adopt the *J* aggregation mode (where molecules stack by a head-to-tail arrangement). These results are in contrast to those found for phenoxy-substituted heteroleptic and homoleptic bis(phthalocyaninato) holmium(III) counterparts with *H*-aggregation mode (where molecules stack by a face-to-face arrangement), suggesting that bulky naphthoxy substituted side groups would favor packing of adjacent molecules in parallel so that the bulky side groups avoid proximity and minimize steric hindrance. It should be noted that along with the increase in the number of bulky naphthoxy substituents from compound **1** to **2**, the extent of red-shift for the main Q band only slighly increases, implying the steric hindrance of bulky naphthoxy substituents has a great influence on the intermolecular interaction in the self-assemblies.

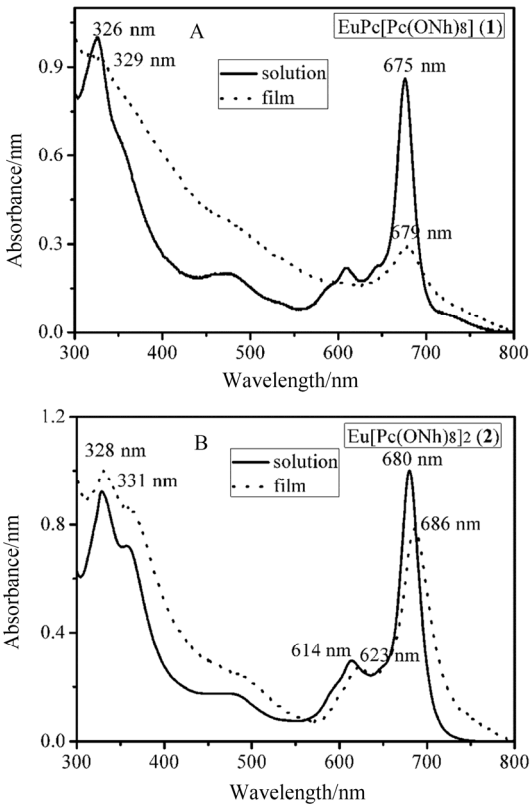

Figure 2 UV-vis absorption spectra of compounds **1** (A) and **2** (B) in DMF solution (solid line) and self-assemblies obtained by QLS method (dot line).

To obtain information of the intermolecular interaction between adjacent molecules, XRD spectra of the self-assemblies of **1** and **2** were recorded in Figure 3. As revealed, in the low angle range, the XRD diagram of the self-assemblies formed from **1** shows a strong refraction peak at $2\theta=4.32°$ (corresponding to 2.05 nm), which is ascribed to the diffraction from the (001) plane. In addition, two clear diffraction peaks at $2\theta=6.13°$ (1.44 nm) and $2\theta=9.78°$ (0.90 nm) are also presented, respectively, originating from the (010) and (100) planes. It is noteworthy that an additional diffraction appeared at 0.32 nm in the wide angle region, which should be attributed to the π-π stacking distance between the phthalocyanine rings without the naphthoxy group of neighboring double-decker molecules along the direction perpendicular to the phthalocyanine rings.[29,30] These three diffraction peaks in the low angle range should be assigned to diffraction from a parallelepiped lattice with the cell parameters of $a=2.05$ nm (length), $b=1.44$ nm (width) and $c=0.90$ nm (thickness), the inset of Figure 3A, formed from edge-to-edge (*J*-type) stacking of two double-decker molecules depending on the π-π stacking and the van der Waals intermolecular interactions between neighboring double-decker molecules on the basis of the energy-optimized, dimensional

CHINESE JOURNAL OF CHEMISTRY

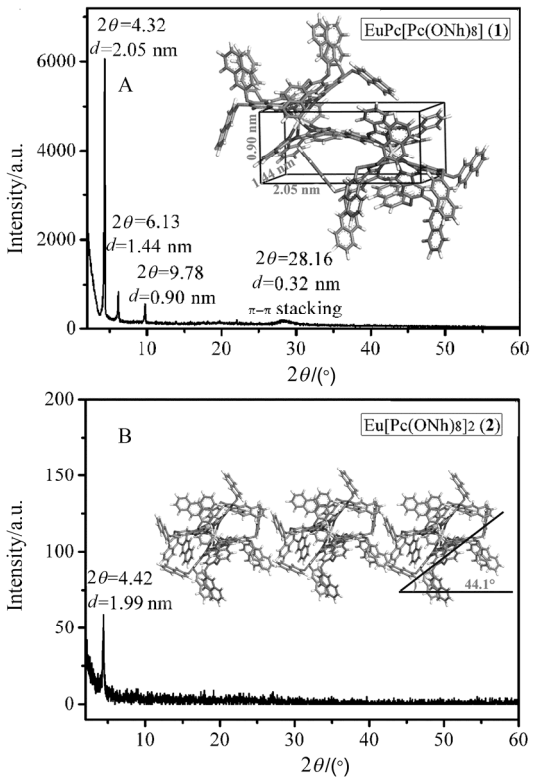

Figure 3 X-ray diffraction patterns of the self-assemblies of compounds **1** (A) and **2** (B). The insets are schematic packing modes.

size for the double-decker EuPc[Pc(ONh)$_8$] (**1**) [2.86 nm (diameter)×0.60 nm (height)] using PCMODEL for windows Version 6.0, Serena Software. As for the self-assemblies of Eu[Pc(ONh)$_8$]$_2$ (**2**), the XRD diagram shows only one peak at 1.99 nm in the low angle range, Figure 3B, corresponding to the thickness of one layer of the film, suggesting the lamellar film-structure formed.[31,32] As a result, a structural transformation from the parallelepiped lattice to the lamellar structure is achieved by increasing the number of naphthoxy groups attached onto the periphery of the Pc rings for the double-decker complex. Judging from the diagonal dimension of the compound **2** molecule obtained on the basis of the energy-optimized molecular structure, 2.86 nm, the orientation angle between the phthalocyanine ring in the double-decker molecule and substrate surface is calculated to amount to *ca*. 44.1°. This is in line with the calculated result (43.9°) based on the polarized UV-vis spectroscopy according to a literature method,[33] Figure S2 and Table S2 (Supporting Information). Consequently, the double-decker molecules of **2** are oriented nearly parallel to the substrate surface in *J*-aggregation mode with an "edge-on" conformation of the double-decker molecules in the film (inset of Figure 3). This is in line with the UV-vis measurement results (*vide supra*). Moreover, the intensity of the (001) peak at 2θ= 4.32° for **1** increased remarkably, compared to that for **2**, indicating a higher crystallinity for self-assembled nanostructure of **1**. The favorable π-π stacking interaction among the double-decker molecules together with enhanced crystallinity for the self-assemblies of **1** is believed to provide the π electrons (or holes) with an extensive area for delocalization, thus favoring charge transport. In the case of the self-assemblies of **2**, only (001) diffraction peak is observed without the presence of an obvious π-π stacking feature, which will negatively impact on the charge transports, as discussed further below.

AFM images can provide more information on the aspect of the self-assemblies and therefore allow us to correlate the morphology and electrical properties. As revealed in Figure 4A, the images for the self-assemblies of **1** show uniform small grain crystallites with approximately 100 nm in diameter. A root-mean-square (Rrms) roughness value of 1.06 nm is revealed, implying a typical smooth surface for the self-assemblies of **1**. On the other hand, some disconnected domains with *ca*. (150±15) nm in size were observed for the self-assemblies of **2**, Figure 4B, giving a relatively high Rrms value of 2.65 nm. The more uniform grain size and much lower Rrms value for the self-assemblies of **1** compared to those of **2** is expected to cause fewer traps and/or defects localized around grain boundaries, thus improving the electrical conductivity and gas sensing as detailed below.

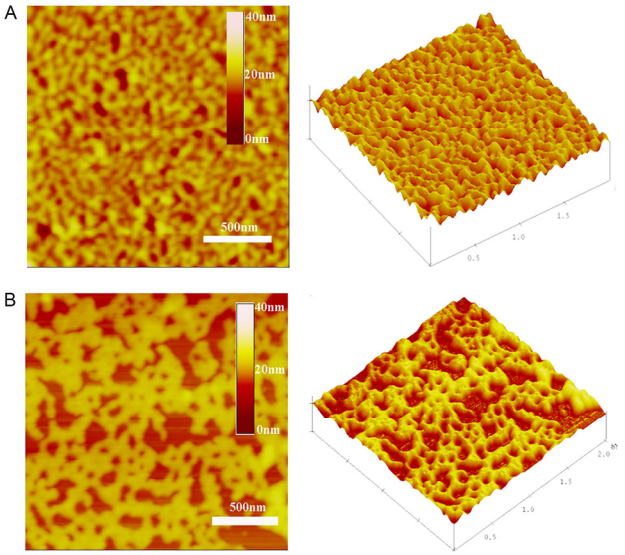

Figure 4 AFM images and corresponding 3D enlarged images for the self-assemblies of **1** (A) and **2** (B).

Electrical and sensing properties

The electron conductivity measurements were conducted by *I-V* curves for the self-assemblies of **1**—**2**. As shown in Figure 5, both two devices exhibit similar Ohmic behavior at low bias voltage, confirming the good electrical contact between the organic self-assemblies and electrodes. However, current response decreased significantly along with the increase in the number of naphthoxy groups of the macrocycles from **1** to **2**, with the calculated electronic conductivity about (2.07±0.5)×10^{-5} and (6.79±0.5)×10^{-6} S•cm^{-1} for the

aggregates of **1** and **2**, respectively. Comparing with that of **2**, the improved conductivity of self-assemblies of **1** might be attributed to both readily π-stacks with adjacent EuPc[Pc(ONh)$_8$] molecules and higher ordered molecular arrangement from reducing the steric hindrance of bulky naphthoxy substituents in addition to the fewer traps and/or defects in the self-assemblies of **1**. This result suggested that the number of substituent groups plays a critical role in tuning the intermolecular stacking, and then impacts on electrical conductivity of materials.

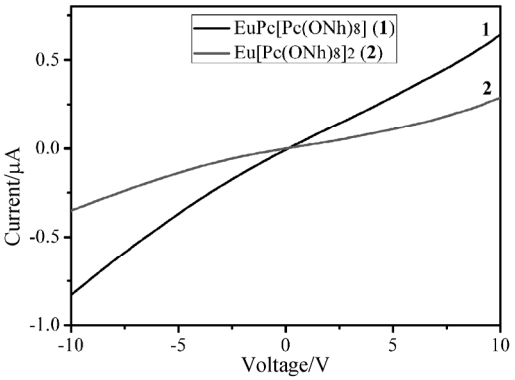

Figure 5 *I-V* curves measured on the self-assemblies of **1** and **2**.

To assess the applicability of gas sensing of double-decker complexes **1**—**2**, the devices fabricated based on the self-assemblies of **1**—**2** were exposed to different concentration of electron-accepting gas NO_2 (50—250 ppb for **1**, 0.5—1.5 ppm for **2**) and electron-donating gas NH_3 (2.5—12.5 ppm for **1**, 25—250 ppm for **2**) in N_2 atmosphere at room temperature. The sensing performances were studied with a duty cycle where the dynamic exposure period was fixed at 5 min for NO_2 and 3 min for NH_3. The responses to NO_2 and NH_3 for the self-assemblies of **1** and **2** were recorded, Figure 6. As can be seen qualitatively in Figure 6A, the current of the self-assemblies of **1** decreased during exposure to 50—250 ppb NO_2 and increased during recovery, which is consistent with the sensing behavior reported previously for *n*-type semiconductors.[34,35] Indeed, NO_2 is a strong oxidizing agent, which generates additional positive charge carriers in EuPc[Pc(ONh)$_8$], and in turn leads to a decrease in electron concentration (majority charge carriers for *n*-type semiconductors). Interestingly, upon exposure to the electron-donating gas NH_3 in 2.5—12.5 ppm range, the conductivity of the self-assemblies of **1** still decreased, Figure 6B, as the behaviors for *p*-type semiconductors.[5,11] When electron-donating NH_3 molecules are absorbed on the surface of the *p*-type semiconductors, the hole concentration of the surface will be weakened since NH_3 traps majority charge carriers (holes), resulting in the decrease in conductivity.[36] Therefore, ambipolar (*n*- and *p*-type) response towards oxidizing NO_2 and reducing NH_3 was revealed for the self-assemblies of **1**. To the best of our knowledge, this is the first example of ambipolar charge-transporting gas sensing devices fabricated from single-component organic semiconductors. However, when the self-assemblies of **2** were exposed to 0.5—1.5 ppm NO_2, the conductivity significantly decreased, exactly as expected for an *n*-type semiconductor, Figure 6C. In addition, the sensors fabricated from the self-assemblies of **2** were totally insensitive to both 50–250 ppb NO_2 applied for **1** and 25—250 ppm NH_3 (whose concentration is above ten times higher than that used for **1)**, Figure 6D. The poor sensing response of **2** should mainly be ascribed to the existence of steric hindrance, thus either a small amount of NO_2 or much more NH_3 molecules adsorbed on the surface of the self-assemblies have little contributions to the conductivity.

In order to quantitatively analyze the sensor responses, the percent current change was calculated for each concentration, as follows:

$$\%\ \text{current change} = [(I_f - I_0)/I_0] \times 100 \quad (2)$$

where I_0 is the current at the start of an exposure/rest cycle and I_f is the current at the end of the exposure period. The values are designated as the sensor response at given NO_2 and NH_3 concentrations as depicted in Figures 6E and 6F. It can be seen that for both self-assemblies of **1** and **2**, the responses are fitting nonlinear curves with respect to analyte concentration (in general $R^2 \geqslant 0.98$). From the equations of the curves as shown in Figures 6E—F, the slopes are decreased gradually as the concentrations of the analytes increase, which mean both compounds **1** and **2** are more sensitive to low concentrations of both NO_2 and NH_3, which is important for the application as gas sensing and/or detector. However, further increasing the concentration of the analyte led to a lower sensitivity. Specially, the response gradually approached the saturated status to the relatively high concentration of analyte. This implied that the much more analyte molecules have completely filled the adsorption sites of the semiconducting layer and the redundant gases have little contribution to the conductivity of the films. Similar behaviors have been reported for MPc-based sensors.[11,36,37] By comparing the value of the slope, EuPc[Pc(ONh)$_8$] is more sensitive to analytes than Eu[Pc(ONh)$_8$]$_2$. The results show that both conductivity and microstructure of self-assemblies have significant effect on the sensing characteristics. The better electric conductivity, higher crystallinity and larger specific surface area for the self-assemblies of **1** than those of **2** render it excellent sensing property for either electron-accepting gas NO_2 in the 50—250 ppb range or electron-donating gas NH_3 in the 2.5—12.5 ppm range due to the optimized molecular packing in the uniform-sized nanoparticles depending on the effective intermolecular interaction between double-decker molecules. The results are inter esting since we can easily detect concentration of NH_3 well below the requirements for detection in industrial wastes control (~10

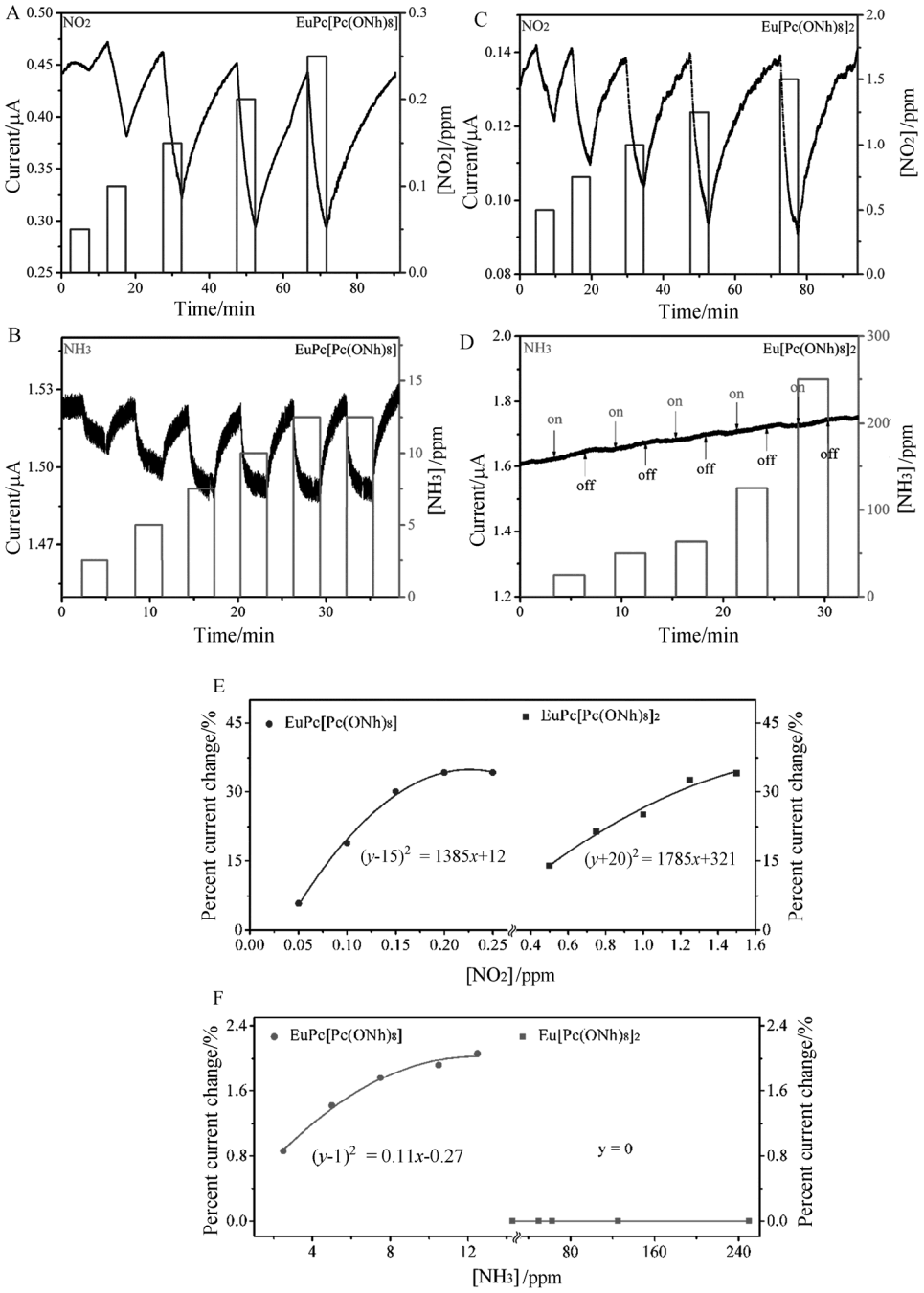

Figure 6 The time-dependent current plots (A—D) and relative response of sensors as a function of the analyte concentration (E—F) for the self-assemblies of **1** and **2** exposed to NO_2 and NH_3 (A, B for **1**, C, D for **2**) at varied concentration in N_2 atmosphere.

ppm NH_3) at room temperature. Furthermore, the lowest NO_2 detection limit of 50 ppb has also met the required standard for national primary ambient air quality (~50 ppb NO_2) in China.

Conclusions

Heteroleptic and homoleptic bis(phthalocyaninato) europium semiconductors Eu(Pc)[Pc(ONh)$_8$] (**1**) and Eu[Pc(ONh)$_8$]$_2$ (**2**) with different number of bulky electro-withdrawing naphthoxy substituents at the periphery of phthalocyanine rings are designed and synthesized. Their LUMO and HOMO levels are successfully tuned into the required range for ambipolar organic semiconductors. Using solution-processed QLS method, self-assemblies with different microstructure and morphology were obtained, with an optimized molecular packing in the uniform-sized nanoparticles and high crystallinity for **1** and disconnected nanograin domains with large gaps and cracks for **2**, depending on the competition and cooperation between the intermolecular π–π interaction, the van der Waals forces and steric hindrance of the bulky naphthoxy groups between neighboring double-decker molecules. The self-assemblies of **1** are more sensitive to both NO_2 and NH_3 relative to

those of **2**, with the detection limit as low as 50 ppb for NO_2 and 2.5 ppm for NH_3, respectively, implying inherently good gas sensing properties of the bis(phthalocyaninato) rare earth double-decker complex. Meanwhile, self-assemblies of **1** exhibited *n*-type response to NO_2 and *p*-type response to NH_3, while only *n*-type performance was obtained to strong oxidant gas NO_2 for the self-assemblies of **2**. The present work opens a new way for the preparation of high-performance ambipolar chemical sensors through the combination of molecular design and solution-based self-assembled technique.

Acknowledgement

We are thankful for financial support from the National Natural Science Foundation of China (Nos. 21371073 and 21290174), the National Key Basic Research Program of China (Nos. 2013CB933402 and 2012CB224801), the Fundamental Research Funds for the Central Universities (No. 16CX06022A) and Research Fund for Introduced Talents of China University of Petroleum (No.Y1510051).

References

[1] Andre, J. J.; Simon, J. *Molecular Semiconductors*, Spring-Verlag, Berlin, **1985**.
[2] Bouvet, M. *Anal. Bioanal. Chem.* **2006**, *384*, 366.
[3] Bouvet, M.; Leroy, A.; Simon, J.; Tournilhac, F.; Guillaud, G.; Lessnick, P.; Maillard, A.; Spirkovitch, S.; Debliquy, M.; de Haan, A.; Decroly, A. *Sens. Actuators B* **2001**, *72*, 86.
[4] Pauly, A.; Bouvet, M. *Encyclopedia of Sensors* **2006**, *6*, 227.
[5] Sizun, T.; Bouvet, M.; Chen, Y.; Suisse, J. M.; Barochi, G.; Rossignol, J. *Sens. Actuators B* **2011**, *159*, 163.
[6] Bao, Z.; Lovinger, A. J.; Brown, J. *J. Am. Chem. Soc.* **1998**, *120*, 207.
[7] Jiang, J.; Ng, D. K. P. *Acc. Chem. Res.* **2009**, *42*, 79.
[8] Bouvet, M.; Xiong, H.; Parra, V. *Sens. Actuators B* **2010**, *145*, 501.
[9] Parra, V.; Brunet, J.; Pauly, A.; Bouvet, M. *Analyst* **2009**, *134*, 1776.
[10] Kılınc, N.; Atilla, D.; Gürek, A. G.; Öztürk, Z. Z.; Ahsen, V. *Sens. Actuators B* **2009**, *142*, 73.
[11] Chen, Y.; Li, D.; Yuan, N.; Gao, J.; Gu, R.; Lu, G.; Bouvet, M. *J. Mater. Chem.* **2012**, *22*, 22142.
[12] Kong, X.; Zhang, X.; Gao, D.; Qi, D.; Chen, Y.; Jiang, J. *Chem. Sci.* **2015**, *6*, 1967.
[13] Lu, G.; Bai, M.; Li, R.; Zhang, X.; Ma, C.; Lo, P. C.; Ng, D. K. P.; Jiang, J. *Eur. J. Inorg. Chem.* **2006**, *18*, 3703.
[14] Kong, X.; Jia, Q.; Wu, F.; Chen, Y. *Dyes Pigm.* **2015**, *115*, 67.
[15] Zhao, Y.; Ding, J.; Huang, X.-B. *Chin. Chem. Lett.* **2014**, *25*, 46.
[16] Chen, Y.; Bouvet, M.; Sizun, T.; Gao, Y.; Plassard, C.; Lesniewska, E.; Jiang, J. *Phys. Chem. Chem. Phys.* **2010**, *12*, 12851.
[17] Ahn, A.; Chandekar, A.; Kang, B.; Sung, C.; Whitten, J. E. *Chem. Mater.* **2004**, *16*, 3274.
[18] Ma, P.; Kan, J.; Zhang, Y.; Huang, C.; Bian, Y.; Chen, Y.; Kobayashi, N.; Jiang, J. *J. Mater. Chem.* **2011**, *21*, 18552.
[19] Zhu, P.; Lu, F.; Pan, N.; Arnold, D. P.; Zhang, S.; Jiang, J. *Eur. J. Inorg. Chem.* **2004**, *3*, 510.
[20] Gobeze, H. B.; Tram, T.; KC, C. B.; Cantu, R. R.; Karr, P. A.; D'Souza, F. *Chin. J. Chem.* **2016**, DOI:10.1002/cjoc.201600403.
[21] Tang, M. L.; Reichardt, A. D.; Wei, P.; Bao, Z. *J. Am. Chem. Soc.* **2009**, *131*, 5264.
[22] Kan, J.; Chen, Y.; Qi, D.; Liu, Y.; Jiang, J. *Adv. Mater.* **2012**, *24*, 1755.
[23] Gao, D.; Zhang, X.; Kong, X.; Chen, Y.; Jiang, J. *ACS Appl. Mater. Interfaces* **2015**, *7*, 2486.
[24] Li, D.; Wang, H.; Kan, J.; Lu, W.; Chen, Y.; Jiang, J. *Org. Electron.* **2013**, *14*, 2582.
[25] Gao, D.; Zhang, X.; Luan, J.; Chen, Y. *Inorg. Chem. Commun.* **2015**, *54*, 50.
[26] Markovitsi, D.; Tran-Thi, T. H.; Even, R.; Simon, J. *Chem. Phys. Lett.* **1987**, *137*, 107.
[27] Zhang, Y.; Cai, X.; Zhou, Y.; Zhang, X.; Xu, H.; Liu, Z.; Li, X.; Jiang, J. *J. Phys. Chem. A* **2007**, *111*, 392.
[28] Kasha, M.; Rawls, H. R.; El-Bavoumi, M. A. *Pure Appl. Chem.* **1965**, *11*, 371.
[29] Lu, G.; Chen, Y.; Zhang, Y.; Bao, M.; Bian, Y.; Li, X.; Jiang, J. *J. Am. Chem. Soc.* **2008**, *130*, 11623.
[30] Lu, G.; Kong, X.; Ma, P.; Wang, K.; Chen, Y.; Jiang, J. *ACS Appl. Mater. Interfaces* **2016**, *8*, 6174.
[31] Liu, J. F.; Yang, K. Z.; Lu, Z. H. *J. Am. Chem. Soc.* **1997**, *119*, 11061.
[32] Xiao, K.; Liu, Y.; Yu, G.; Zhu, D. *Appl. Phys. A* **2003**, *77*, 367.
[33] Yoneyama, M.; Sugi, M.; Saito, M.; Ikegami, K.; Kuroda, S. i.; Iizima, S. *Jpn. J. Appl. Phys.* **1986**, *25*, 961.
[34] Wu, Y.; Ma, P.; Liu, S.; Chen, Y. *New J. Chem.* **2016**, *40*, 3323.
[35] Yang, R. D.; Park, J.; Colesniuc, C. N.; Schuller, I. K.; Royer, J. E.; Trogler, W. C.; Kummel, A. C. *J. Chem. Phys.* **2009**, *130*, 164703.
[36] Gao, J.; Lu, G.; Kan, J.; Chen, Y.; Bouvet, M. *Sens. Actuators B* **2012**, *166—167*, 500.
[37] Bohrer, F. I.; Sharoni, A.; Colesniuc, C.; Park, J.; Schuller, I. K.; Kummel, A. C.; Trogler, W. C. *J. Am. Chem. Soc.* **2007**, *129*, 5640.

(Zhao, X.)

